


## Article

# Novel Red Light-Absorbing Organic Dyes Based on Indolo[3,2-b]carbazole as the Donor Applied in Co-Sensitizer-Free Dye-Sensitized Solar Cells

Zhanhai Xiao <sup>1,2</sup>, Bing Chen <sup>2,\*</sup>  and Xudong Cheng <sup>1,\*</sup>

<sup>1</sup> State Key Laboratory of Advanced Technology for Materials Synthesis and Processing, Wuhan University of Technology, Wuhan 430070, China; xiaozhanhai@whut.edu.cn

<sup>2</sup> State Key Laboratory of Magnetic Resonance and Atomic and Molecular Physics, Innovation Academy for Precision Measurement Science and Technology, Chinese Academy of Science, Wuhan 430071, China

\* Correspondence: chenbing@wipm.ac.cn (B.C.); xudong.cheng@whut.edu.cn (X.C.); Tel.: +86-134-7621-3393 (B.C.)

**Abstract:** Three novel organic dyes (**D6**, **D7** and **D8**), based on indolo[3,2-b]carbazole as the donor and different types of electron-withdrawing groups as the acceptors, were synthesized and successfully applied in dye-sensitized solar cells (DSSCs). Their molecular structures were fully characterized by <sup>1</sup>H NMR, <sup>13</sup>C NMR and mass spectroscopy. The density functional theory (DFT) calculations, electrochemical impedance spectroscopy analysis, UV–Vis absorption characterization and tests of the solar cells were used to investigate the photophysical/electrochemical properties as well as DSSCs' performances based on the dyes. Dye **D8** showed the broadest light-response range (300–770 nm) in the incident monochromatic photo-to-electron conversion efficiency (IPCE) curve, due to its narrow bandgap (1.95 eV). However, dye **D6** exhibited the best device performance among the three dyes, with power conversion efficiency of 5.41%,  $J_{sc}$  of 12.55 mA cm<sup>-2</sup>,  $V_{oc}$  of 745 mV and fill factor (FF) of 0.59. We also found that dye aggregation was efficiently suppressed by the introduction of alkylated indolo[3,2-b]carbazole, and, hence, better power conversion efficiencies were observed for all the three dyes, compared to the devices of co-sensitization with chenodeoxycholic acid (CDCA). It was unnecessary to add adsorbents to suppress the dye aggregation.

**Keywords:** organic dyes; indolo[3,2-b]carbazole; DFT calculations; dye aggregation; benzothiadiazole



**Citation:** Xiao, Z.; Chen, B.; Cheng, X. Novel Red Light-Absorbing Organic Dyes Based on Indolo[3,2-b]carbazole as the Donor Applied in Co-Sensitizer-Free Dye-Sensitized Solar Cells. *Materials* **2021**, *14*, 1716. <https://doi.org/10.3390/ma14071716>

Academic Editor: Gregory J. Wilson

Received: 9 February 2021

Accepted: 23 March 2021

Published: 31 March 2021

**Publisher's Note:** MDPI stays neutral with regard to jurisdictional claims in published maps and institutional affiliations.



**Copyright:** © 2021 by the authors. Licensee MDPI, Basel, Switzerland. This article is an open access article distributed under the terms and conditions of the Creative Commons Attribution (CC BY) license (<https://creativecommons.org/licenses/by/4.0/>).

## 1. Introduction

In the past three decades, scientists have paid much attention to the dye-sensitized solar cells (DSSCs). They have been regarded as an alternative energy source since the first report in 1991, due to their ability to convert solar energy to electricity at a low cost and excellent photovoltaic performance [1–4]. To date, Ru-complex and Zn-porphyrin sensitizers have achieved high power conversion efficiencies (PCEs) of 11.9% and 13.5%, respectively [5,6]. However, the high cost, limited resource of ruthenium and the complex synthesis procedure of zinc porphyrin impede their further application in DSSCs. Therefore, worldwide scientists have been involved in developing metal-free organic dyes with high PCE, due to their flexible structural modification, simple synthesis, low toxicity and low cost [7,8]. Recently, DSSCs based on metal-free organic dyes have achieved a very high PCE of 14% [9]. However, those dyes have complex structures and are difficult to synthesize. In addition, they need particular electrolytes and a co-sensitizer to improve open circuit voltage and suppress the dye aggregation to achieve high PCE. These reasons work against the commercialization of dyes. Therefore, the organic dyes featuring simple synthesis and without the necessity for using a co-sensitizer to improve PCE in the DSSCs could be a promising research field.

Among various metal-free organic dyes, the dyes with donor– $\pi$ –bridge–acceptor (D– $\pi$ –A) structures exhibit outstanding performance with simple molecular structures.

For the typical D- $\pi$ -A dyes, the structural modifications of the donor and acceptor can effectively tune the energy levels and improve intramolecular charge transfer (ICT) from D to A, therefore providing a direct way for acquiring high PCE [10]. Many kinds of promising donors have been reported, such as carbazole [11–15], di(1-benzothieno)[3,2-b:2',3'-d]pyrrole [16,17], triphenylamine [18], dithieno[3,2-b]pyrrolobenzotriazole [19], and so on. Recently, indolo[3,2-b]carbazole featuring a larger conjugated plane than triphenylamine and carbazole has been reported as an excellent donor to construct organic optoelectronic functional materials, due to its outstanding hole-donating ability [20,21]. With its high thermal and chemical stability, indolo[3,2-b]carbazole was proven to be a good candidate as the D unit of organic dyes [22]. We previously reported a series of efficient D-D- $\pi$ -A organic dyes based on indolo[3,2-b]carbazole as the first donor [23,24], triphenylamine as the second donor, and thiophene cyanoacetic acid as the acceptor, showing efficient photovoltaic performance with a highest PCE up to 6.34%. That study indicated that indolo[3,2-b]carbazole was a potential donor group in D-D- $\pi$ -A-type organic dyes. However, it was rarely reported that indolo[3,2-b]carbazole was used as a single donor group. The study focus on the behaviors of indolo[3,2-b]carbazole-based D- $\pi$ -A and D-A- $\pi$ -A dyes is also an interesting field. In addition, the light-response ranges based on previously reported dyes were not satisfactory, because they can only absorb the visible light, which leads to comparably low PCE, compared with those near-infrared-absorbing organic dyes. To expand the light absorption to longer wavelengths, an excellent acceptor should be introduced to the dyes to enhance the D- $\pi$ -A effects. We found that 2,1,3-benzothiadiazole as promising electron acceptor plays a crucial role in power conversion efficiency [25,26]. Because of its strong electron withdrawing ability, benzothiadiazole could lower the energy level of the lowest unoccupied molecular orbital (LUMO) and further reduce the energy gap of sensitizers [27,28]. Therefore, benzothiadiazole may be a suitable acceptor and is easily connected by some well-performed donors to enhance dye performances with simple dye structures.

In this work, we synthesized three dyes (D6, D7 and D8) by adopting indolo[3,2-b]carbazole as single donor to simplify synthesis and thiophene cyanoacetic acid, benzothiadiazole benzoic acid and benzothiadiazole thiophene cyanoacetic acid as respective acceptors to modify the bandgap of dyes. The structures of D6–D8 were shown in Figure 1. As the results show, the introduction of benzothiadiazole effectively expanded the light absorption of dyes to 690 nm. In addition, the dye aggregation was also suppressed by the two alkyl chains of indolo[3,2-b]carbazole, demonstrating better PCE even in the co-sensitizer-free DSSCs. Finally, the systematic study of their photophysical and electrochemical properties, as well as the resulting DSSCs performances based on the three dyes, was also reported.

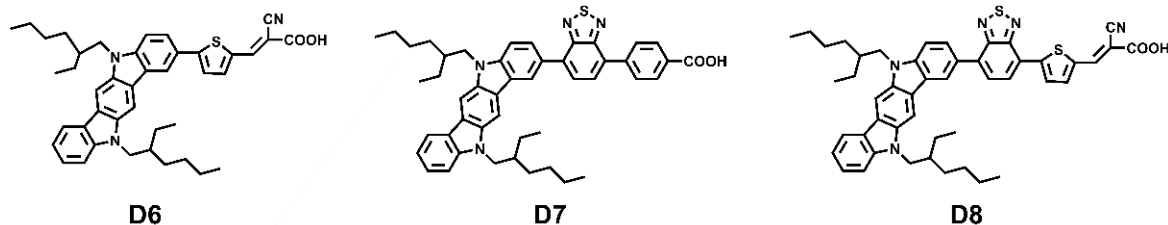


Figure 1. The structures of the new dyes.

## 2. Experimental

### 2.1. Materials and Methods

All the chemicals used in this study were purchased from Sigma–Aldrich (Saint Louis, MO, USA) and J&K Chemical Ltd (Beijing, China). The solvents used in synthesis were purified using standard processes. The reactions in this study were carried out in the N<sub>2</sub>

atmosphere. The separation of the compounds was carried out on column chromatography using silica gel (200–300 mesh).

Nuclear Magnetic Resonance (NMR) spectra ( $^1\text{H}$  and  $^{13}\text{C}$ ) characterization were tested on a Bruker 500 MHz spectrometer in  $\text{CDCl}_3$  and  $\text{DMSO-}d_6$ . Mass spectra were carried out on a Bruker microTOF-Q. The absorption spectra of dyes were recorded on a HP 8453 spectrophotometer. Electrochemical properties were studied by cyclic voltammetry measurements on a CHI604D electrochemical workstation, using  $\text{Bu}_4\text{NPF}_6$  as supporting electrolyte, dry dichloromethane as solvent and  $\text{N}_2$  as protection gas. The scan rate was  $50 \text{ mV s}^{-1}$ . The ferrocene/ferrocenium ( $\text{Fc}/\text{Fc}^+$ ) redox couple was used as the internal standard. The current voltage (J–V) tests of the DSSCs were carried out on Keithley 2400 source meter under simulated AM 1.5 G ( $100 \text{ mW cm}^{-2}$ ) illumination with a solar light simulator. Incident monochromatic photo-to-electron conversion efficiency (IPCE) was measured from 300 to 800 nm by a Spectral Products DK240 monochromator. The electrochemical impedance spectra (EIS) were carried out on a CHI604D electrochemical work station under dark conditions.

## 2.2. Fabrication and Characterization of DSSCs

Nanocrystalline  $\text{TiO}_2$  films were prepared by screen printing two kinds of  $\text{TiO}_2$  nanoparticles (a  $12 \mu\text{m}$  nanoporous layer and a  $4 \mu\text{m}$  scattering layer) over the conductive side of the conducting glass. The active area of the  $\text{TiO}_2$  was  $0.196 \text{ cm}^2$ . The photoanode was prepared by immersing the  $\text{TiO}_2$  film into a  $0.3 \text{ mM}$  dye solution in THF for 24 h under the dark. After the dye adsorption, the photoanode was washed with dichloromethane (DCM) and then dried. The electrolyte contained acetonitrile–valeronitrile (85:15, v/v), composed of  $0.6 \text{ M}$  BMII (1-butyl-3-methylimidazolium iodide),  $0.05 \text{ M}$  LiI,  $0.03 \text{ M}$   $\text{I}_2$ ,  $0.5 \text{ M}$  4-tert-butylpyridine and  $0.1 \text{ M}$  guanidinium thiocyanate. The electrolyte was inserted into the interspace between the photoanode and cathode from the two holes predrilled on the back of the counter electrode. At last, the holes were sealed with a Surlyn film and a thin glass.

## 2.3. Synthesis

Synthetic routes to the three dyes **D6**, **D7** and **D8** are depicted in Scheme 1. Compound **1** was prepared via substitution reaction of 5,11-Dihydroindolo[3,2-b]carbazole with 2-ethylhexyl bromide and NaOH in DMSO, according to the literature [29]. Compound **1** was prepared by controlling the amount of N-bromosuccinimide (NBS) to provide monobrominated compound **2**. Then, key intermediate compounds, such as pinacol boronic ester **2**, were afforded by coupling bis(pinacolato)diboron with compound **3**. Compounds **5**, **6**, **3a**, **3b** and **3c** were synthesized by Suzuki coupling reaction. The dyes **D6** and **D8** were synthesized by condensation of aldehydes **3a** and **3c** with piperidine cyanoacetic acid. Dye **D7** was synthesized by hydrolysis of compound **3b** in sodium hydroxide solution. The NMR and mass spectra of **D6–D8** are shown in Figures S1–S6.

### 2-bromo-5,11-bis(2-ethylhexyl)-5,11-dihydroindolo[3,2-b]carbazole (**2**)

In a  $100 \text{ mL}$  flask, compound **1** ( $2.3 \text{ g}$ ,  $4.8 \text{ mmol}$ ) was dissolved in  $40 \text{ mL}$  THF solution and stirred at  $0 \text{ }^\circ\text{C}$  for 15 min. Under light-shielding conditions, ( $937 \text{ mg}$ ,  $5.2 \text{ mmol}$ ) N-bromosuccinimide (NBS) was added portion-wise. After 2 h of reaction, the temperature was gradually raised to room temperature, and the reaction was continued for 24 h. The reaction mixture was poured into water and extracted with DCM, and the combined extracts were washed with water and dried with anhydrous  $\text{NaSO}_4$ . The solvent was removed with a rotary evaporator, and the residue was isolated by silica gel column chromatography with petroleum ether (PE) as eluent to afford compound **2** as a yellow–green solid (yield: 81%,  $2.17 \text{ g}$ ).  $^1\text{H}$  NMR ( $\text{CDCl}_3$ , 600 MHz, ppm):  $\delta$  8.27 (d,  $J = 1.8 \text{ Hz}$ , 1H), 8.19 (d,  $J = 7.8 \text{ Hz}$ , 1H), 7.92 (s, 1H), 7.83 (s, 1H), 7.53–7.48 (m, 2H), 7.38 (d,  $J = 8.4 \text{ Hz}$ , 1H), 7.25–7.21 (m, 2H), 4.19–4.12 (m, 4H), 2.17–2.12 (m, 2H), 1.48–1.29 (m, 16H), 0.97–0.90 (m, 12H).  $^{13}\text{C}$  NMR ( $\text{CDCl}_3$ , 150 MHz, ppm):  $\delta$  142.37, 140.76, 140.74, 136.72, 128.11, 126.03, 124.65, 123.43, 122.79, 122.71, 121.54, 120.25, 118.09, 110.54, 110.11, 108.84, 99.12, 99.01, 47.83,

47.81, 39.40, 39.34, 31.20, 31.16, 28.97, 28.94, 24.64, 23.26, 23.21, 14.24, 14.22, 11.14, 11.12. HRMS (ESI, m/z): [M]<sup>+</sup> calcd for [C<sub>34</sub>H<sub>43</sub>BrN<sub>2</sub>]<sup>+</sup>: 558.2610, found: 558.2630.

### **5,11-bis(2-ethylhexyl)-2-(4,4,5,5-tetramethyl-1,3,2-dioxaborolan-2-yl)-5,11-dihydroindolo[3,2-b]carbazole (3)**

In a 250 mL flask, compound 2 (2 g, 3.57 mmol), bis(pinacolato)diboron (B<sub>2</sub>pin<sub>2</sub>) (2.72 g, 10.72 mmol), anhydrous potassium acetate (KOAc) (1.05 g, 10.72 mmol) and dichloro[1,1'-bis(diphenylphosphino)-ferrocene]palladium(II) (Pd(dppf)Cl<sub>2</sub>) (261 mg, 0.357 mmol) were dissolved in 100 mL degassed dioxane under N<sub>2</sub> atmosphere. The reaction was stirred at 80 °C for 24 h. Then, water was added and extracted with DCM. The organic layer was combined and dried with anhydrous NaSO<sub>4</sub>. The solvent was removed under vacuum, and the crude compound was purified by column chromatography with PE:DCM = 1:1 as the eluent to give brown viscous oil compound 3 (yield: 69%, 1.50 g). <sup>1</sup>H NMR (CDCl<sub>3</sub>, 500 MHz, ppm): δ 8.70 (s, 1H), 8.20 (d, *J* = 7.7 Hz, 1H), 8.07 (s, 1H), 7.99 (s, 1H), 7.95 (d, *J* = 8.5 Hz, 1H), 7.49–7.46 (m, 1H), 7.42–7.38 (m, 2H), 7.25–7.22 (m, 1H), 4.33–4.23 (m, 4H), 2.24–2.18 (m, 2H), 1.43 (s, 12H), 1.41–1.26 (m, 16H), 0.97–0.94 (m, 6H), 0.91–0.88 (m, 6H). <sup>13</sup>C NMR (CDCl<sub>3</sub>, 125 MHz, ppm): 144.40, 142.13, 136.83, 136.45, 134.82, 132.25, 131.34, 127.76, 127.45, 125.61, 122.83, 120.04, 117.91, 108.72, 108.09, 99.33, 98.93, 83.62, 47.72, 39.21, 31.02, 28.84, 25.05, 24.48, 23.23, 14.11, 11.05. HRMS (ESI, m/z): [M]<sup>+</sup> Calcd. for (C<sub>40</sub>H<sub>55</sub>BN<sub>2</sub>O<sub>2</sub>), 606.4357, found: 606.4369.

### **methyl 4-(7-bromobenzo[c][1,2,5]thiadiazol-4-yl)benzoate (5)**

(4-(methoxycarbonyl)phenyl)boronic acid (1 g, 5.5 mmol), 4,7-dibromobenzo[c][1,2,5]thiadiazole (1.96 g, 6.6 mmol), Pd(PPh<sub>3</sub>)<sub>4</sub> (321 mg, 0.27 mmol), THF (150 mL) and 2 M K<sub>2</sub>CO<sub>3</sub> (50 mL) were added in a 250 mL flask under N<sub>2</sub> atmosphere. After stirring at 80 °C for 8 h, the mixture was extracted with DCM and removed under reduced pressure. The residue was isolated by silica gel column chromatography with PE:DCM = 1:1 as the eluent to give faint yellow solid compound 5 (780 mg, 41%). <sup>1</sup>H NMR (CDCl<sub>3</sub>, 500 MHz, ppm): 8.21 (d, *J* = 8.4 Hz, 2H), 8.00 (d, *J* = 8.0 Hz, 2H), 7.97 (d, *J* = 7.2 Hz, 1H), 7.65 (d, *J* = 7.6 Hz, 1H), 3.98 (s, 3H). <sup>13</sup>C NMR (CDCl<sub>3</sub>, 125 MHz, ppm): 166.77, 153.91, 152.88, 140.94, 132.84, 132.19, 130.12, 129.95, 129.17, 128.79, 114.25, 52.31. HRMS (ESI, m/z): [M + H]<sup>+</sup> Calcd. for (C<sub>14</sub>H<sub>10</sub>BrN<sub>2</sub>O<sub>2</sub>S), 348.9646, found: 348.9651.

### **5-(7-bromobenzo[c][1,2,5]thiadiazol-4-yl)thiophene-2-carbaldehyde (6)**

Compound 4 (0.5 g, 3.2 mmol), 4,7-dibromobenzo[c][1,2,5]thiadiazole (1.41 g, 4.8 mmol), Pd(PPh<sub>3</sub>)<sub>4</sub> (321 mg, 0.27 mmol), THF (50 mL) and 2 M K<sub>2</sub>CO<sub>3</sub> (50 mL) were added in a 100 mL flask under N<sub>2</sub> atmosphere. The reaction solution was refluxed for 12 h. The resulting mixture was extracted with DCM and washed with distilled water. The organic layer was dried with anhydrous NaSO<sub>4</sub>. The solvent was removed under vacuum, and the crude compound was purified by column chromatography with PE:DCM = 1:1 as the eluent to give compound 6 (yield: 35%, 364 mg). <sup>1</sup>H NMR (CDCl<sub>3</sub>, 500 MHz, ppm): 10.03 (s, 1H), 8.21 (d, *J* = 4.2 Hz, 1H), 7.96 (d, *J* = 7.8 Hz, 1H), 7.88 (d, *J* = 4.1 Hz, 1H), 7.86 (d, *J* = 7.5 Hz, 1H), <sup>13</sup>C NMR (CDCl<sub>3</sub>, 125 MHz, ppm): 182.99, 147.56, 143.95, 136.67, 134.05, 132.14, 131.35, 128.54, 127.37, 125.75, 115.11. HRMS (ESI, m/z): [M]<sup>+</sup> Calcd. for (C<sub>11</sub>H<sub>5</sub>BrN<sub>2</sub>OS<sub>2</sub>), 323.9027, found: 323.9011.

### **5-(5,11-bis(2-ethylhexyl)-5,11-dihydroindolo[3,2-b]carbazol-2-yl)thiophene-2-carbaldehyde (3a)**

Compound 3 (300 mg, 0.49 mmol), compound 4 (92 mg, 0.59 mmol), Pd(PPh<sub>3</sub>)<sub>4</sub> (46 mg, 0.04 mmol), THF (30 mL) and 2 M K<sub>2</sub>CO<sub>3</sub> (1 mL) were added in a 100 mL flask under N<sub>2</sub> atmosphere. The reaction solution was refluxed for 12 h. The resulting mixture was extracted with DCM and washed with distilled water. The organic layer was dried with anhydrous NaSO<sub>4</sub>. The solvent was removed under vacuum, and the crude compound was purified by column chromatography with PE:DCM = 1:1 as the eluent to give compound 3a (yield: 51%, 149 mg). <sup>1</sup>H NMR (CDCl<sub>3</sub>, 500 MHz, ppm): 9.89 (s, 1H), 8.47 (s, 1H), 8.20 (d, *J* = 7.80 Hz, 1H), 7.99 (s, 2H), 7.76–7.80 (m, 2H), 7.52–7.46 (m, 2H), 7.25–7.22 (m, 2H),

4.40–4.32 (m, 4H), 2.18–2.08 (m, 2H), 1.41–1.26 (m, 16H), 0.91–0.86 (m, 6H), 0.80–0.75 (m, 6H).  $^{13}\text{C}$  NMR ( $\text{CDCl}_3$ , 125 MHz, ppm): 183.13, 164.45, 155.45, 148.32, 145.16, 142.36, 142.09, 136.95, 133.45, 132.35, 126.71, 124.66, 123.73, 123.06, 122.89, 122.17, 121.03, 118.11, 110.34, 109.63, 99.73, 47.43, 38.99, 30.59, 28.34, 24.37, 23.45, 14.33, 11.12. HRMS (ESI, m/z):  $[\text{M}]^+$  Calcd. for ( $\text{C}_{39}\text{H}_{46}\text{N}_2\text{OS}$ ), 590.3331, found: 590.3316.

**methyl 4-(7-(5,11-bis(2-ethylhexyl)-5,11-dihydroindolo[3,2-b]carbazol-2-yl)benzo[c][1,2,5]thiadiazol-4-yl)benzoate (3b)**

Compound **3** (300 mg, 0.49 mmol), compound **5** (207 mg, 0.59 mmol),  $\text{Pd}(\text{PPh}_3)_4$  (46 mg, 0.04 mmol), THF (30 mL) and 2 M  $\text{K}_2\text{CO}_3$  (1 mL) were added in a 100 mL flask under  $\text{N}_2$  atmosphere. The reaction solution was refluxed for 12 h. The resulting mixture was extracted with DCM and washed with distilled water. The organic layer was dried with anhydrous  $\text{NaSO}_4$ . The solvent was removed under vacuum, and the crude compound was purified by column chromatography with PE:DCM = 1:1 as the eluent to give compound **3b** (yield: 39%, 144 mg).  $^1\text{H}$  NMR ( $\text{CDCl}_3$ , 500 MHz, ppm): 8.95 (s, 1H), 8.37 (s, 1H), 8.31 (s, 1H), 8.28 (d,  $J = 7.56$  Hz, 1H), 8.22 (d,  $J = 8.50$  Hz, 2H), 8.18 (d,  $J = 8.50$  Hz, 2H), 8.13 (d,  $J = 8.40$  Hz, 2H), 8.08 (s, 2H), 7.68 (d,  $J = 8.66$  Hz, 2H), 7.52 (d,  $J = 8.26$  Hz, 1H), 7.47–7.43 (m, 1H), 7.21–7.16 (m, 1H), 4.42–4.34 (m, 4H), 3.90 (s, 3H), 2.20–2.09 (m, 2H), 1.44–1.16 (m, 16H), 0.93–0.73 (m, 12H).  $^{13}\text{C}$  NMR ( $\text{CDCl}_3$ , 125 MHz, ppm): 166.71, 154.23, 153.82, 142.10, 136.82, 136.71, 134.97, 130.04, 129.84, 128.04, 127.11, 123.02, 122.80, 122.67, 109.50, 100.23, 52.73, 47.33, 35.58, 31.72, 30.64, 29.43, 28.44, 24.22, 23.01, 14.33, 11.27. HRMS (ESI, m/z):  $[\text{M}]^+$  Calcd. for ( $\text{C}_{48}\text{H}_{52}\text{N}_4\text{O}_2\text{S}$ ), 748.3811, found: 748.3826.

**5-(7-(5,11-bis(2-ethylhexyl)-5,11-dihydroindolo[3,2-b]carbazol-2-yl)benzo[c][1,2,5]thiadiazol-4-yl)thiophene-2-carbaldehyde (3c)**

Compound **3** (300 mg, 0.49 mmol), compound **6** (193 mg, 0.59 mmol),  $\text{Pd}(\text{PPh}_3)_4$  (46 mg, 0.04 mmol), THF (30 mL) and 2 M  $\text{K}_2\text{CO}_3$  (1 mL) were added in a 100 mL flask under  $\text{N}_2$  atmosphere. The reaction solution was refluxed for 12 h. The resulting mixture was extracted with DCM and washed with distilled water. The organic layer was dried with anhydrous  $\text{NaSO}_4$ . The solvent was removed under vacuum, and the crude compound was purified by column chromatography with PE:DCM = 1:1 as the eluent to give compound **3c** (yield: 34%, 121 mg).  $^1\text{H}$  NMR ( $\text{CDCl}_3$ , 500 MHz, ppm): 10.02 (s, 1H), 8.82 (d,  $J = 1.65$  Hz, 1H), 8.26 (d,  $J = 4.35$  Hz, 1H), 8.21 (d,  $J = 8.01$  Hz, 1H), 8.16–8.11 (m, 2H), 8.07 (s, 1H), 8.04 (s, 1H), 7.92 (d,  $J = 7.48$  Hz, 1H), 7.87 (d,  $J = 4.04$  Hz, 1H), 7.55 (d,  $J = 8.70$  Hz, 1H), 7.51–7.47 (m, 1H), 7.41 (d,  $J = 8.21$  Hz, 1H), 7.23 (d,  $J = 7.21$  Hz, 1H), 4.38–4.25 (m, 4H), 2.27–2.11 (m, 2H), 1.41–1.16 (m, 16H), 0.90–0.81 (m, 6H), 0.81–0.76 (m, 6H).  $^{13}\text{C}$  NMR ( $\text{CDCl}_3$ , 125 MHz, ppm): 183.11, 154.34, 152.83, 149.27, 143.10, 142.45, 142.19, 136.93, 136.84, 136.38, 127.82, 127.71, 127.12, 126.73, 125.82, 123.70, 123.37, 123.70, 122.72, 121.14, 120.13, 118.02, 108.84, 99.27, 47.87, 39.33, 31.08, 28.86, 24.56, 23.11, 14.12, 11.03. HRMS (ESI, m/z):  $[\text{M}]^+$  Calcd. for ( $\text{C}_{45}\text{H}_{48}\text{N}_4\text{OS}_2$ ), 724.3270, found: 724.3280.

**(E)-3-(5-(5,11-bis(2-ethylhexyl)-5,11-dihydroindolo[3,2-b]carbazol-2-yl)thiophen-2-yl)-2-cyanoacrylic acid (D6)**

Compound **3a** (100 mg, 0.17 mmol), cyanoacetic acid (43 mg, 0.75 mmol), piperidine (101 g, 1.18 mmol) and chloroform (30 mL) were added in a 100 mL flask under  $\text{N}_2$  atmosphere. The reaction solution was refluxed for 12 h. After that, the resulting mixture was acidified with 2 M HCl aqueous solution (40 mL) for 0.5 h. The resulting mixture was extracted with DCM and washed with distilled water. The organic layer was dried with anhydrous  $\text{NaSO}_4$ . The solvent was removed under vacuum, and the crude compound was purified by column chromatography with MeOH:DCM = 1:10 as the eluent to give dye **D6** (yield: 80%, 89 mg).  $^1\text{H}$  NMR ( $\text{CDCl}_3$ , 500 MHz, ppm): 8.72 (s, 1H), 8.46 (s, 1H), 8.42 (d,  $J = 5.2$  Hz, 1H), 8.29 (d,  $J = 7.5$  Hz, 2H), 8.03 (d,  $J = 3.8$  Hz, 1H), 7.88 (d,  $J = 8.0$  Hz, 1H), 7.79–7.78 (m, 1H), 7.63–7.60 (m, 1H), 7.53 (d,  $J = 8.0$  Hz, 1H), 7.48–7.46 (m, 1H), 7.22–7.18 (m, 1H), 4.40–4.32 (m, 4H), 2.18–2.08 (m, 2H), 1.41–1.26 (m, 16H), 0.91–0.86 (m, 6H), 0.80–0.75 (m, 6H).  $^{13}\text{C}$  NMR ( $\text{CDCl}_3$ , 125 MHz, ppm): 164.41, 155.85, 142.66, 142.15, 136.82, 133.73,

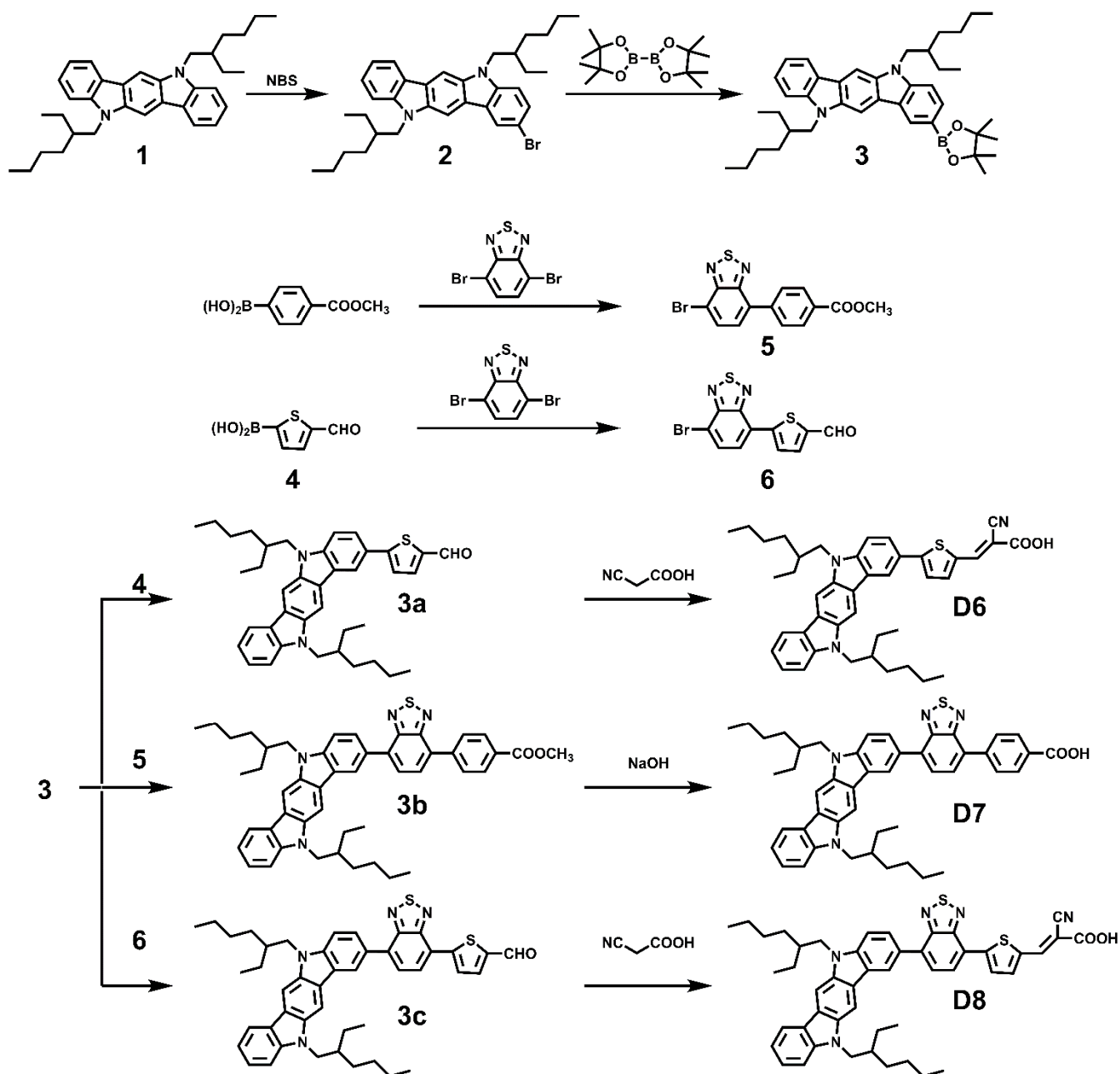
126.41, 124.09, 123.45, 123.06, 122.49, 122.23, 120.94, 118.82, 110.34, 109.5, 100.60, 100.40, 47.31, 38.91, 30.51, 28.56, 24.32, 23.31, 14.20, 11.00. HRMS (ESI, m/z):  $[M - H]^-$  Calcd. for ( $C_{42}H_{47}N_3O_2S$ ), 656.3312, found: 657.3303.

**methyl 4-(7-(5,11-bis(2-ethylhexyl)-5,11-dihydroindolo[3,2-b]carbazol-2-yl)benzo[c][1,2,5]thiadiazol-4-yl)benzoate (D7)**

Compound **3b** (100 mg, 0.13 mmol), NaOH aqueous solution (9.5 mL, 20%), MeOH (15 mL) and THF (30 mL) were added in a 100 mL flask. After that, the resulting mixture was acidified with 2 M HCl aqueous solution (40 mL) for 0.5 h. The resulting mixture was extracted with DCM and washed with distilled water. The organic layer was dried with anhydrous  $NaSO_4$ . The solvent was removed under vacuum, and the crude compound was purified by column chromatography with MeOH:DCM = 1:10 as the eluent to give dye **D7** (yield: 75%, 74 mg).  $^1H$  NMR ( $CDCl_3$ , 500 MHz, ppm): 8.68 (s, 1H), 8.25–8.21 (m, 3H), 8.06 (d,  $J = 8.20$  Hz, 3H), 8.01 (s, 1H), 7.95 (s, 1H), 7.78–7.70 (m, 2H), 7.53–7.49 (m, 1H), 7.43–7.36 (m, 2H), 7.29–7.26 (m, 1H), 4.31–4.01 (m, 4H), 2.28–2.09 (m, 2H), 1.49–1.26 (m, 16H), 1.01–0.96 (m, 6H), 0.92–0.87 (m, 6H).  $^{13}C$  NMR ( $CDCl_3$ , 125 MHz, ppm): 171.92, 154.41, 153.83, 142.76, 142.18, 136.83, 136.66, 135.48, 130.41, 130.30, 129.13, 128.87, 128.51, 127.14, 126.91, 125.74, 123.16, 122.91, 122.80, 121.00, 120.11, 117.98, 108.67, 99.16, 47.69, 39.32, 31.08, 28.87, 24.50, 23.09, 14.14, 11.03. HRMS (ESI, m/z):  $[M - H]^-$  Calcd. for ( $C_{47}H_{50}N_4O_2S$ ), 733.3582, found: 733.3575.

**(E)-3-(5-(7-(5,11-bis(2-ethylhexyl)-5,11-dihydroindolo[3,2-b]carbazol-2-yl)benzo[c][1,2,5]thiadiazol-4-yl)thiophen-2-yl)-2-cyanoacrylic acid (D8)**

The synthetic method of the dye **D8** was similar with that of the compound **D6**, and the residue was isolated by silica gel column chromatography with MeOH:DCM = 1:8 as the eluent to give orange solid dye **D8** (yield: 78%, 85 mg).  $^1H$  NMR (DMSO, 500 MHz, ppm): 8.88 (s, 1H), 8.33–8.27 (m, 3H), 8.25–8.22 (m, 2H), 8.18 (s, 1H), 8.12 (d,  $J = 8.52$  Hz, 1H), 7.99 (d,  $J = 7.52$  Hz, 1H), 7.83 (d,  $J = 3.76$  Hz, 1H), 7.57–7.53 (m, 2H), 7.49–7.46 (m, 1H), 7.22–7.19 (m, 1H), 4.36–4.29 (m, 4H), 2.18–2.11 (m, 2H), 1.41–1.16 (m, 16H), 0.90–0.81 (m, 3H), 0.81–0.76 (m, 9H).  $^{13}C$  NMR (DMSO, 125 MHz, ppm): 164.31, 154.34, 152.56, 150.61, 149.11, 143.45, 142.03, 138.59, 136.74, 136.62, 131.89, 131.16, 130.11, 128.01, 127.41, 126.81, 126.28, 125.71, 123.71, 122.98, 122.65, 118.31, 117.18, 115.94, 109.41, 100.15, 47.27, 38.99, 30.51, 28.40, 24.32, 22.98, 14.35, 11.24. HRMS (ESI, m/z):  $[M]^+$  Calcd. for ( $C_{48}H_{49}N_5O_2S_2$ ), 791.3322, found: 791.3340.



Scheme 1. Synthetic routes of the dyes.

### 3. Results and Discussion

#### 3.1. Photophysical Properties

The UV–Visible absorption spectra of dyes **D6**, **D7** and **D8** in DCM solution with concentration of  $1 \times 10^{-5}$  M are presented in Figure 2, and the corresponding data are listed in Table 1. The shorter wavelengths located at 300–370 nm are ascribed to the localized  $\pi$ – $\pi^*$  transitions of the conjugated backbone, while the band of 400–600 nm is attributed to the intramolecular charge transfer (ICT) transition from donor to acceptor [30,31]. The maximum absorption wavelength ( $\lambda_{max}$ ) for dyes **D6**, **D7** and **D8** are 500 nm, 463 nm and 529 nm, respectively. Dyes **D6–D8** show molar extinction coefficient ( $\epsilon$ ) with values of around  $4.59 \times 10^4$  M<sup>-1</sup>cm<sup>-1</sup>,  $1.58 \times 10^4$  M<sup>-1</sup>cm<sup>-1</sup> and  $1.73 \times 10^4$  M<sup>-1</sup>cm<sup>-1</sup>, respectively. The remarkably high  $\epsilon$  of dye **D6** is due to the introduction of a thiophene group, which expand the conjugate plane. Therefore, the light absorption properties of dye **D6** have

been improved [32,33]. In addition, a larger  $\epsilon$  allows a thinner TiO<sub>2</sub> film, which shortens the electrolyte diffusion distance in the film and, thus, reduces the charge recombination during transport [24]. Furthermore, dye **D8** shows the broadest absorption band of the dyes, and the  $\lambda_{max}$  red-shifted about 87 nm and 21 nm, in comparison with dyes **D6** and **D7**, respectively, due to its stronger ICT transition.

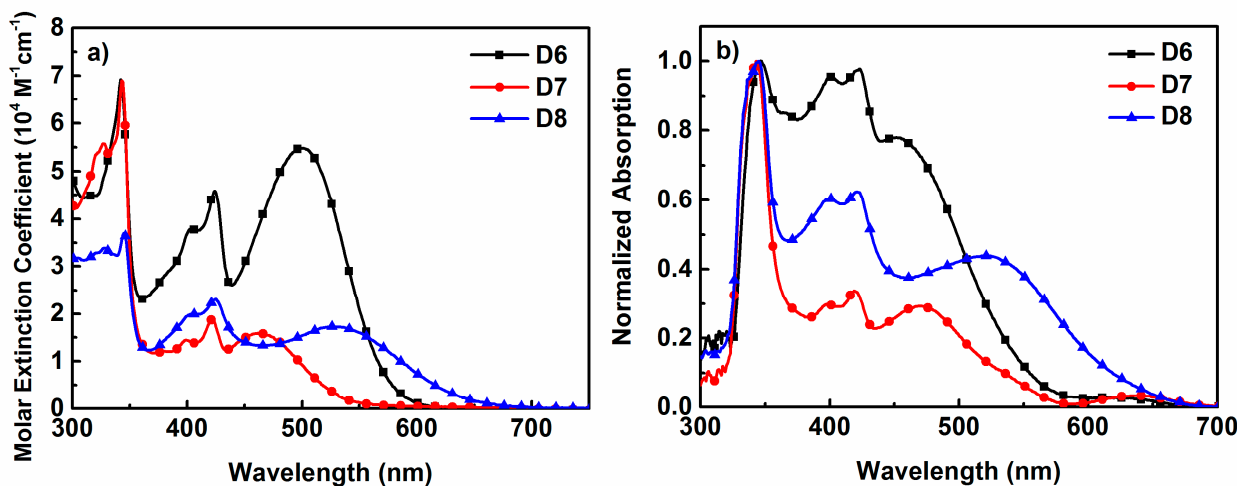


Figure 2. (a) Absorption spectra of dyes in DCM solution. (b) Absorption spectra of dyes on TiO<sub>2</sub> film.

Table 1. Photophysical and Electrochemical properties of the dyes.

Dye	$(\lambda_{max}^{[a]} \text{ nm}/\epsilon^{[a]} \text{ M}^{-1}\text{cm}^{-1})$	$E_{0-0}^{[b]}$ (eV)	$E_{ox}^{[c]}$ (V)	$E_{red}^{[d]}$ (V)	$G_{inj}^{[e]}$ (eV)	$G_{reg}^{[f]}$ (eV)
<b>D6</b>	404 ( $3.79 \times 10^4$ ), 424 ( $4.59 \times 10^4$ ), 500 ( $5.48 \times 10^4$ )	2.17	0.87	−1.30	−0.80	−0.47
<b>D7</b>	399 ( $1.44 \times 10^4$ ), 421 ( $1.87 \times 10^4$ ), 463 ( $1.58 \times 10^4$ )	2.36	1.01	−1.35	−0.85	−0.61
<b>D8</b>	404 ( $1.99 \times 10^4$ ), 425 ( $2.31 \times 10^4$ ), 529 ( $1.73 \times 10^4$ )	1.95	0.81	−1.08	−0.58	−0.41

<sup>[a]</sup> The maximum absorption wavelength ( $\lambda_{max}$ ) and molar extinction coefficients ( $\epsilon$ ). <sup>[b]</sup>  $E_{0-0}$  was calculated from  $E_{0-0} = 1240/\lambda_{onset}$ , where  $\lambda_{onset}$  was determined from the onset of absorption spectrum. <sup>[c]</sup> The oxidation potential versus NHE, which was calculated by  $E_{ox}[\text{V}] = E_{ox}(\text{vs. Fc/Fc}^+) + 0.63$ . <sup>[d]</sup>  $E_{red}[\text{V}] = E_{ox} - E_{0-0}$ . <sup>[e]</sup> Driving force for electron injection from dye-excited state into the conduction band of TiO<sub>2</sub> (−0.5 V vs. NHE). <sup>[f]</sup> Driving force for dye regeneration by the  $\text{I}^-/\text{I}_3^-$  redox shuttle (+0.4 V vs. NHE).

The normalized absorption spectra of dyes **D6–D8** adsorbed on 12  $\mu\text{m}$  TiO<sub>2</sub> films are shown in Figure 2b. After being anchored onto the TiO<sub>2</sub> films, the absorption spectra (300–750 nm) of the three dyes were wider, compared with the spectra in solution (300–700 nm), which is beneficial to light-harvesting and  $J_{sc}$  enhancement. Compared with the  $\lambda_{max}$  in solution, the  $\lambda_{max}$  of dyes **D6–D8** on TiO<sub>2</sub> film are blue-shifted by about 49, 1 and 8 nm, respectively. The blue-shift of absorption on TiO<sub>2</sub> film is mainly attributed to the deprotonation of carboxylic acid and H-type aggregation [34].

### 3.2. Electrochemical Properties

Electrochemical properties of dyes **D6–D8** were studied by cyclic voltammetry (CV) curves in dichloromethane solution, with TBAPF<sub>6</sub> as the electrolyte. The CV curves are shown in Figure 3a, and the corresponding data are displayed in Table 1. The three dyes show quasireversible oxidation waves, which indicate that the electrochemical properties of these dyes are stable. The oxidative potential ( $E_{ox}$ ) versus normal hydrogen



electrode (vs. NHE) of dyes **D6–D8** are 0.87, 1.01 and 0.81 V, respectively, which are higher than the  $I^-/I_3^-$  potential (+0.4 V), indicating that the oxidized dyes can be regenerated effectively [11,35–37]. The energy gaps ( $E_{0-0}$ ) of dyes **D6–D8**, calculated according to UV–Vis absorption spectra, were 2.17, 2.36 and 1.95 eV, respectively. Therefore, the reductive potentials of dyes **D6–D8**, calculated according to the equation of  $E_{red}[V] = E_{ox} - E_{0-0}$ , were  $-1.30$ ,  $-1.35$  and  $-1.08$  V (vs. NHE), respectively, which are much higher than the conduction-band edge of  $TiO_2$  ( $-0.5$  V). This indicates that the driving force for the electron injection from dyes to the  $TiO_2$  film is sufficient. Figure 3b intuitively illustrates the energy-level distribution of three dyes and the flow direction of electrons in the device.

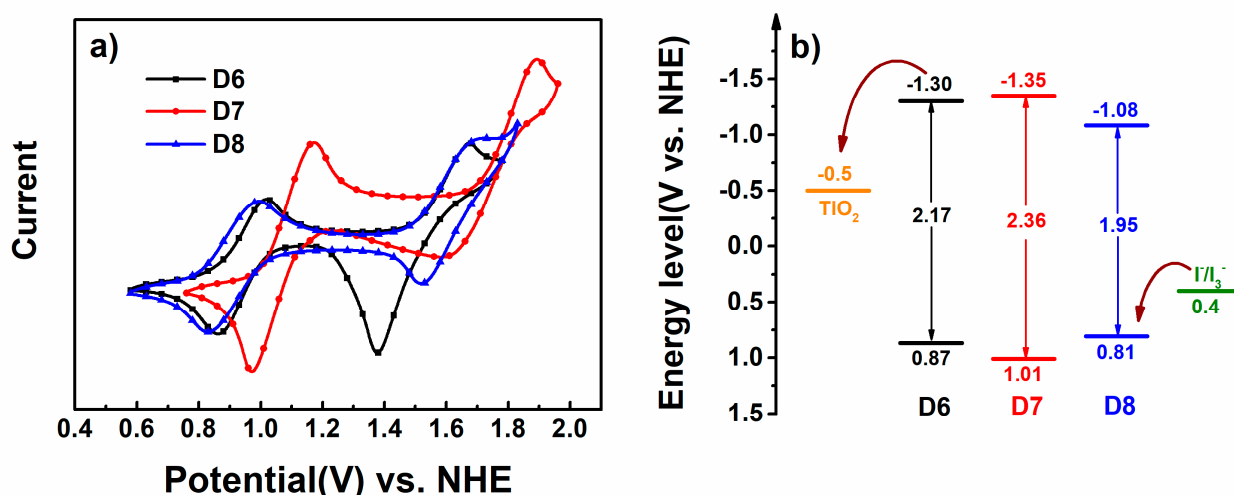


Figure 3. (a) Cyclic voltammograms of the dyes. (b) The energy level diagram of the dyes.

### 3.3. Theoretical Calculations

The structures of dyes **D6–D8** have been further analyzed by using (B3LYP/6-31G (d, p) level). The electron distributions in the highest occupied molecular orbital (HOMOs) and lowest unoccupied molecular orbital (LUMOs) of dyes **D6–D8** are shown in Table 2. The HOMOs of dyes **D6–D8** reside mostly on the indolo[3,2-b] carbazole, and the LUMOs reside over the thiophene, benzothiadiazole and cyanoacrylic acid acceptor. We can observe the significant overlapping between the HOMOs (indolo[3,2-b] carbazole) and LUMOs (thiophene and benzothiadiazole), which facilitates charge transfer transition from the donor to the acceptor. It is worth noting that the electron density of the excited state of dye **D7** is not completely localized at the anchoring units. This unoptimal electronic matching result may influence the electron injection from dye **D7** to the  $TiO_2$  and, thus, cause the unexpectedly lower  $J_{sc}$  recorded. The optimized ground-state geometries (Table 3) indicate that the indolo[3,2-b] carbazole unit presents a rigid planar structure. The dihedral angles (between indolo[3,2-b] carbazole to acceptor) of dyes **D6–D8** are  $21.8^\circ$ ,  $36.0^\circ$  and  $32.7^\circ$ , respectively. The dihedral angle between thiophene and phenyl ( $21.8^\circ$  for dye **D6** and  $0.7^\circ$  for dye **D8**) is smaller than that between two phenyls ( $36^\circ$  for dye **D7** and  $32.7^\circ$  for dye **D8**). This indicates that thiophene group can improve planarity and conjugation, which is good for dye ICT transition [38–40].

Table 2. Optimized molecular geometries and electron distributions of the dyes.

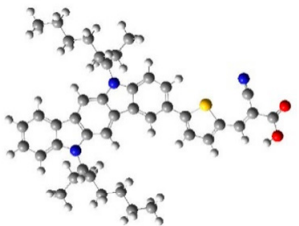
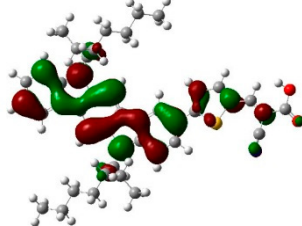
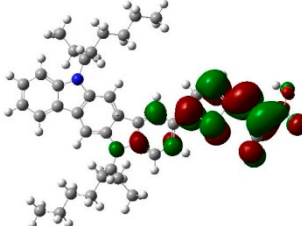
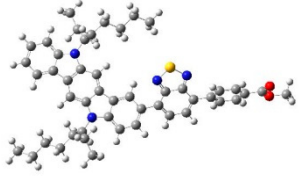
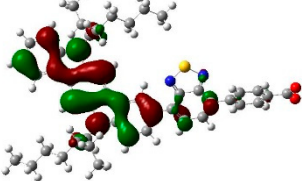
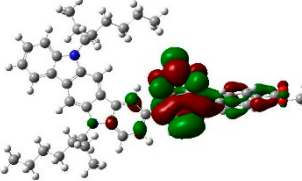
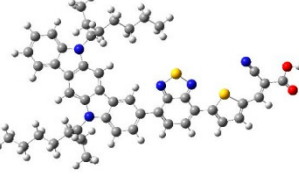
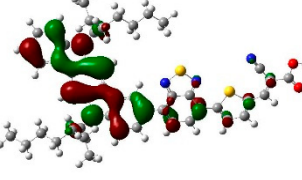
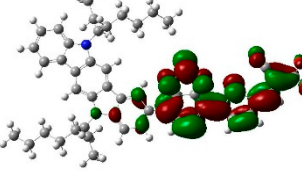
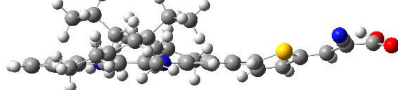
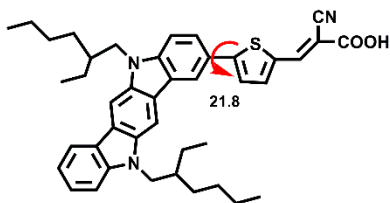
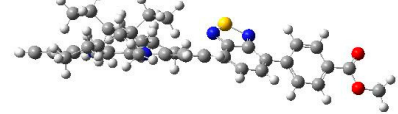
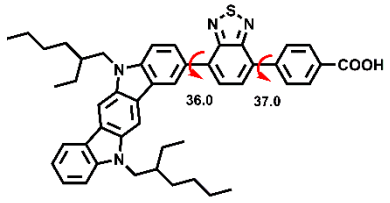
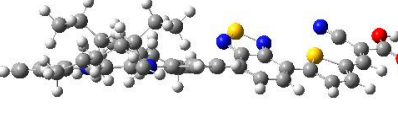
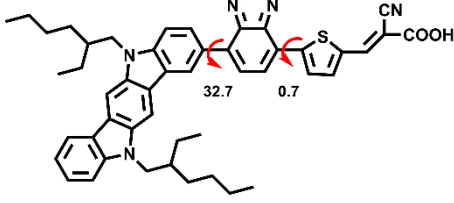
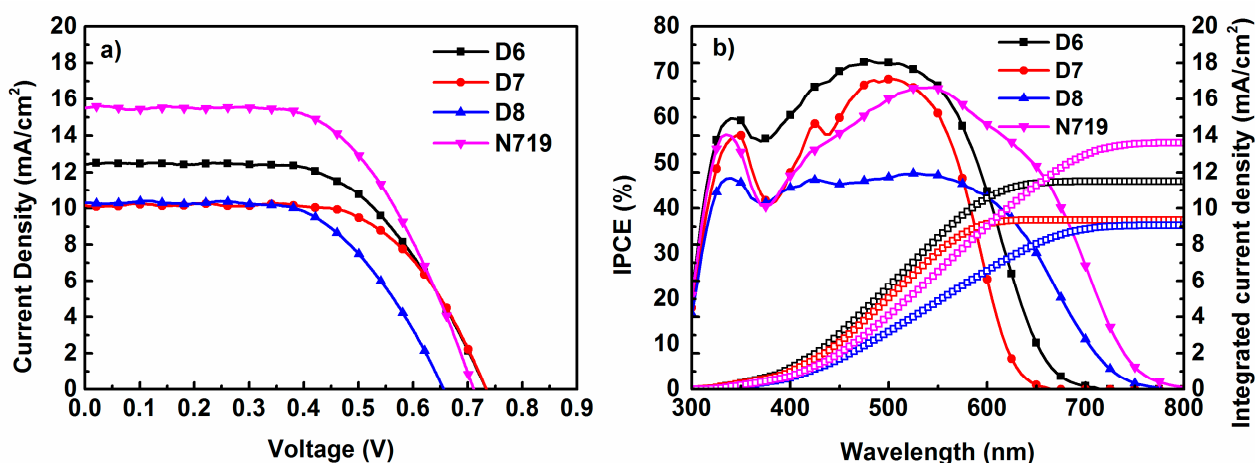
Dyes	Optimized Structure	HOMO	LUMO
D6			
D7			
D8			

Table 3. Dihedral angle and side views of the dyes.

Dye	Side View	Dihedral Angle
D6		
D7		
D8		

### 3.4. Photovoltaic Properties

The photovoltaic properties of dyes **D6–D8** and **N719** are performed under standard conditions (AM 1.5,  $100 \text{ mW cm}^{-2}$ ). The photocurrent–voltage (J–V) curves are shown in Figure 4a, and the corresponding data of short circuit photocurrent density ( $J_{sc}$ ), open-circuit voltage ( $V_{oc}$ ), fill factor (FF) and power conversion efficiency (PCE) are shown in Table 4. In the UV–Visible absorption spectra, dye **D8** shows a broader absorption band, which may lead to a higher  $J_{sc}$ . However, the  $J_{sc}$  of the DSSCs based on dyes **D6–D8** are  $12.55$ ,  $10.76$  and  $10.17 \text{ mA cm}^{-2}$ , respectively. It is clear that the dye **D6**-based cell shows higher  $J_{sc}$  than that of dyes **D7** and **D8**, which is due to its higher molar extinction coefficients. Furthermore, the dye loading amount of dyes **D6–D8** are  $4.16 \times 10^{-7} \text{ mol cm}^{-2}$ ,  $2.81 \times 10^{-7} \text{ mol cm}^{-2}$  and  $2.51 \times 10^{-7} \text{ mol cm}^{-2}$ , respectively, which is consistent with the  $J_{sc}$  of the three dyes. The  $V_{oc}$  of the DSSC based on dyes **D6–D8** is  $745$ ,  $744$  and  $668 \text{ mV}$ , respectively. Compared with the DSSCs of dyes **D7** and **D8**, dye **D6**-based DSSC shows the highest PCE of  $5.41\%$ , due to its high  $J_{sc}$ . Finally, these three dyes exhibit good power conversion efficiency, which indicates that indolo[3,2-b]carbazole group might be a good donor.



**Figure 4.** (a) Photocurrent–voltage curves and (b) incident monochromatic photo-to-electron conversion efficiency (IPCE) spectra and integrated current density of the dye-sensitized solar cells (DSSCs) based on the dyes.

**Table 4.** Photovoltaic parameters of DSSCs based on dyes **D6**, **D7**, **D8** and **N719**.

Dyes	CDCA:Dyes	$J_{sc}/\text{mA cm}^{-2}$	$V_{oc}/\text{mV}$	FF	PCE/%
<b>D6</b>	0:1	12.55	745	0.59	5.41
	3:1	11.55	722	0.59	5.00
	10:1	11.23	718	0.61	4.90
	50:1	10.09	712	0.49	3.50
<b>D7</b>	0:1	10.16	744	0.66	5.01
	3:1	8.65	727	0.64	4.05
	10:1	8.32	738	0.60	3.70
	50:1	7.50	730	0.56	3.09
<b>D8</b>	0:1	10.38	662	0.59	4.03
	3:1	9.87	664	0.59	3.85
	10:1	10.90	671	0.59	4.28
	50:1	9.20	659	0.56	3.40
<b>N719</b>	0	15.40	720	0.59	6.50

The incident photon-to-current conversion efficiency (IPCE) spectra for the cells is shown in Figure 4b. As can be seen, all the three dyes exhibit broad response which indicates that dyes **D6–D8** can convert the visible light to photocurrent efficiently. The

maximum spectra response band of dyes **D6–D8** are at 710, 660 and 770 nm, respectively. The absorption range of dye **D8**-based DSSC is obviously broader than that of dyes **D6** and **D7**, due to the incorporated benzothiadiazole-thiophene unit decreasing the  $E_{0-0}$ . However, dye **D6** shows strong response in the range from 350 to 550 nm, with a highest IPCE value of 72.55% at 480 nm. Dyes **D7** and **D8** display the maximum IPCE values of 68.4% at 500 nm and 47.74% at 525 nm, respectively. Therefore, the best IPCE performance is observed on the dye **D6**, among the three dyes. It mainly originates from its much higher molar extinction coefficient and more dye loading amount. These results are also in good accordance with the  $J_{sc}$  value obtained in above J–V measurements.

The chenodeoxycholic acid (CDCA) co-sensitization was tested by blending dyes **D6**, **D7** and **D8** with different ratios of CDCA in the THF dye bath, respectively. The corresponding curve and data are shown in Figure 5 and Table 4, respectively. Generally, the PCE of most dyes can be improved by the addition of CDCA, because it can restrain the dye aggregation. However, for aggregation-free organic dyes, the addition of CDCA would reduce adsorption of the dye molecules on the  $TiO_2$  film, which would reduce the short-circuit current density and, hence, the power conversion efficiency [41]. The photovoltaic properties of the DSSCs based on dyes **D6–D8** with no additives and with CDCA as co-sensitizer were investigated. As can be seen in Figure 5a,b, the decrease of  $J_{sc}$  is found in dyes **D6**- and **D7**-based DSSC after the co-sensitization. When the ratio of CDCA increases, both the  $J_{sc}$  and PCE of these two dyes decrease. It can be explained that indolo[3,2-b]carbazole and its long alkyl chain can restrain dye aggregation efficiently. Meanwhile, adopting CDCA as the co-adsorbent is unfavorable for these two dyes adsorptions on  $TiO_2$  films. However, Figure 5c shows that  $J_{sc}$  increases by adding 10 times of CDCA. This indicates that **D8** presents aggregation and improved by the addition of CDCA.

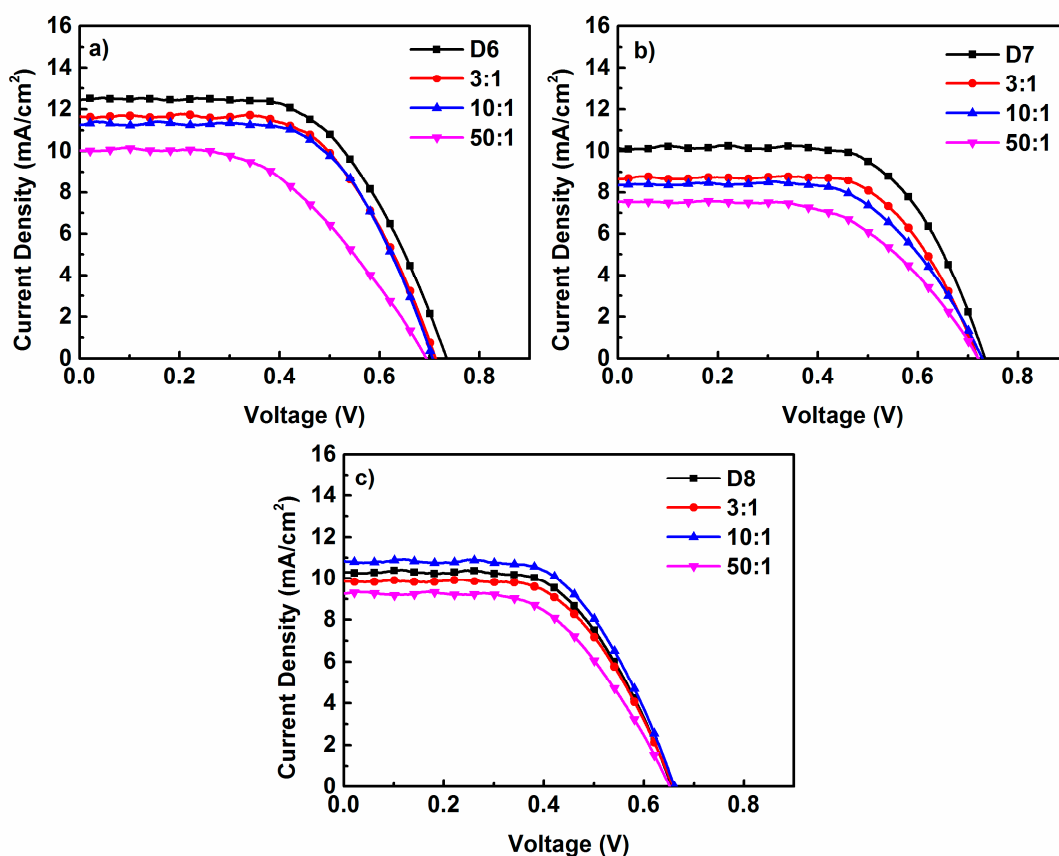


**Figure 5.** (a) J–V curves for the DSSCs based on dye **D6** and co-sensitization of chenodeoxycholic acid (CDCA); (b) J–V curves for the DSSCs based on dye **D7** and co-sensitization of CDCA; (c) J–V curves for the DSSCs based on dye **D8** and co-sensitization of CDCA.

### 3.5. Electrochemical Impedance Spectra (EIS) Analysis

In order to study the charge recombination and charge transfer process in the DSSCs, the electrochemical impedance spectroscopy (EIS) analysis is performed in the dark. The measurement is under a bias of  $-0.7$  V, and the frequency range is 0.1 Hz–10 kHz. The corresponding Nyquist plots are shown in Figure 6a. The first semicircle at higher frequencies corresponds to the electron transport at the Pt/electrolyte interface, and the last one at lower frequencies corresponds to the charge recombination at the  $\text{TiO}_2$ /dyes/electrolyte interface. The larger value of charge transfer resistance ( $R_{ct}$ ) reflects the lower charge recombination, smaller dark current and larger open circuit voltage [42,43]. The values of  $R_{ct}$  can be deduced by fitting curves using ZView complex nonlinear least-square regression software (AMETEK, Leicester, UK). The order of  $R_{ct}$  values is **D8** ( $63.7 \Omega$ ) < **D7** ( $113.0 \Omega$ ) < **D6** ( $155.5 \Omega$ ), which is consistent with the order of  $V_{oc}$  values of **D6** ( $668$  mV) < **D7** ( $744$  mV) < **D8** ( $745$  mV). The electron lifetime ( $\tau$ ) of the dyes **D6–D8** can be calculated from the Bode phase plots (Figure 6b) to support the trends of  $V_{oc}$ . The electron lifetime ( $\tau$ ) is calculated from  $\tau = 1/(2\pi f)$  [44,45], where  $f$  is the peak frequency in lower frequency. The order of  $\tau$  is **D6** ( $25.8$  ms) > **D7** ( $25.5$  ms) > **D8** ( $8.3$  ms), which is in line with their  $V_{oc}$ .

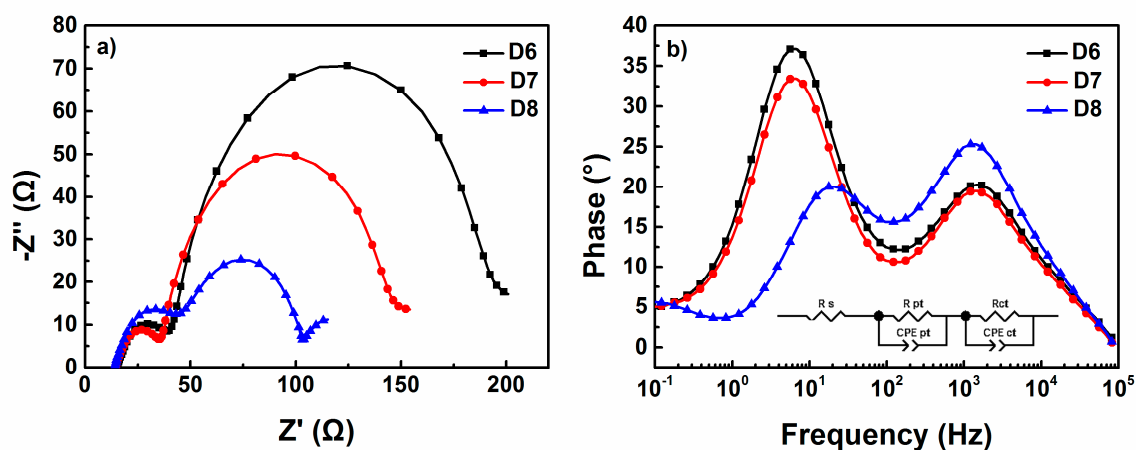


Figure 6. (a) Electrochemical impedance spectra (EIS) Nyquist and (b) Bode plots for DSSCs based on the dyes.

### 3.6. Stability Study

The study of stability of dyes is very important for the DSSCs' applications. The devices, for long term stability, were encapsulated and stored in dark conditions. The evolution of efficiency was measured by testing the PCE values of three DSSCs, based on dyes **D6–D8**, once a day. As we can see in Figure 7, nearly 90% of initial efficiency ( $\eta_0$ ) for all three DSSCs remained over 480 h, which suggests that our dyes are stable and, thus, suggesting application potential.

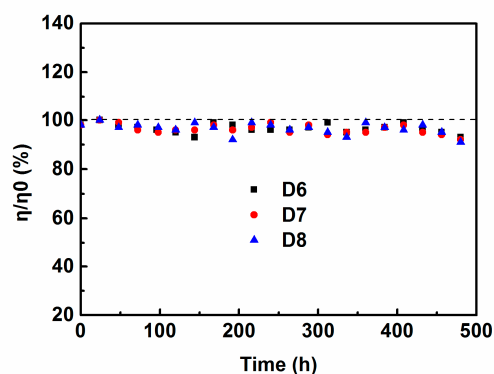


Figure 7. The long-term stability of DSSCs based on the dyes.

#### 4. Conclusions

Three novel metal-free organic dyes (D6, D7 and D8) with different acceptors were synthesized and applied in DSSCs. Dye D6, containing thiophene cyanoacetic acid acceptor, exhibits much higher  $\epsilon$  and dye loading amount than the other two dyes, which indicates that dye D6 possesses better light-harvesting capability. By the adoption of alkylated indolo[3,2-b]carbazole, dye aggregation was efficiently suppressed. Hence, the power conversion efficiencies of the dyes without co-sensitization with CDCA are better, as compared with the co-sensitized devices. Because of the introduction of benzothiadiazole thiophene group, dye D8 shows the broadest light-response range (300–770 nm) in IPCE curve, due to the decrease of the  $E_{0-0}$ . However, its lower  $\epsilon$  and dye loading amount leads to poor photovoltaic performance. The DSSC-based dyes D6–D8 show over 90% of initial efficiency during 480 h. Finally, dye D6 exhibits the best performance among these dyes, with the highest power conversion efficiency of 5.41%, mainly due to its highest  $J_{sc}$  ( $12.55 \text{ mA cm}^{-2}$ ).

**Supplementary Materials:** The following are available online at <https://www.mdpi.com/article/10.3390/ma14071716/s1>, Figure S1.  $^1\text{H}$  NMR of dye D6 in DMSO-d6, Figure S2.  $^1\text{H}$  NMR of dye D7 in  $\text{CDCl}_3$ , Figure S3.  $^1\text{H}$  NMR of dye D8 in DMSO-d6, Figure S5. Mass spectra of dye D6, Figure S5. Mass spectra of dye D7, Figure S6. Mass spectra of dye D8.

**Author Contributions:** Research and writing—original draft preparation, Z.X.; Writing—review and editing, B.C.; Final approval of the version to be published, X.C. All authors have read and agreed to the published version of the manuscript.

**Funding:** This research was funded by the National Natural Science Foundation of China (Nos. 21303256 and 11274347).

**Institutional Review Board Statement:** Not applicable.

**Informed Consent Statement:** Not applicable.

**Data Availability Statement:** Data sharing is not applicable to this article.

**Conflicts of Interest:** The authors declare no conflict of interest.

#### References

1. O'Regan, B.; Grätzel, M. A low-cost, high-efficiency solar cell based on dye-sensitized colloidal  $\text{TiO}_2$  films. *Nature* **1991**, *353*, 737–740. [CrossRef]
2. Grätzel, M. Dye-sensitized solar cells. *J. Photochem. Photobiol. C Photochem. Rev.* **2003**, *4*, 145–153. [CrossRef]
3. Hagfeldt, A.; Boschloo, G.; Sun, L.; Kloo, L.; Pettersson, H. Dye-Sensitized Solar Cells. *Chem. Rev.* **2010**, *110*, 6595–6663. [CrossRef]
4. Gong, J.; Sumathy, K.; Qiao, Q.; Zhou, Z. Review on dye-sensitized solar cells (DSSCs): Advanced techniques and research trends. *Renew. Sustain. Energy Rev.* **2017**, *68*, 234–246. [CrossRef]
5. Mathew, S.; Yella, A.; Gao, P.; Humphry-Baker, R.; Curchod, B.F.E.; Ashari-Astani, N.; Tavernelli, I.; Rothlisberger, U.; Nazeeruddin, M.K.; Grätzel, M. Dye-sensitized solar cells with 13% efficiency achieved through the molecular engineering of porphyrin sensitizers. *Nat. Chem.* **2014**, *6*, 242–247. [CrossRef]
6. Nazeeruddin, M.K.; Kay, A.; Rodicio, I.; Humphry-Baker, R.; Mueller, E.; Liska, P.; Vlachopoulos, N.; Graetzel, M. Conversion of light to electricity by cis-X2bis(2,2'-bipyridyl-4,4'-dicarboxylate)ruthenium(II) charge-transfer sensitizers (X = Cl-, Br-, I-, CN-, and SCN-) on nanocrystalline titanium dioxide electrodes. *J. Am. Chem. Soc.* **1993**, *115*, 6382–6390. [CrossRef]
7. Mishra, A.; Fischer, M.K.R.; Büuerle, P. Metal-Free organic dyes for dye-Sensitized solar cells: From structure: Property relationships to design rules. *Angew. Chem. Int. Ed.* **2009**, *48*, 2474–2499. [CrossRef]
8. Ooyama, Y.; Harima, Y. Molecular designs and syntheses of organic dyes for dye-sensitized solar cells. *Eur. J. Org. Chem.* **2009**, 2903–2934. [CrossRef]
9. Kakiage, K.; Aoyama, Y.; Yano, T.; Otsuka, T.; Kyomen, T.; Unno, M.; Hanaya, M. An achievement of over 12 percent efficiency in an organic dye-sensitized solar cell. *Chem. Commun.* **2014**, *50*, 6379–6381. [CrossRef] [PubMed]
10. Chaurasia, S.; Liang, C.-J.; Yen, Y.-S.; Lin, J.T. Sensitizers with rigidified-aromatics as the conjugated spacers for dye-sensitized solar cells. *J. Mater. Chem. C* **2015**, *3*, 9765–9780. [CrossRef]
11. Zhang, G.; Bai, Y.; Li, R.; Shi, D.; Wenger, S.; Zakeeruddin, S.M.; Grätzel, M.; Wang, P. Employ a bisthienothiophene linker to construct an organic chromophore for efficient and stable dye-sensitized solar cells. *Energy Environ. Sci.* **2009**, *2*, 92–95. [CrossRef]
12. Mariotti, N.; Bonomo, M.; Fagiolari, L.; Barbero, N.; Gerbaldi, C.; Bella, F.; Barolo, C. Recent advances in eco-friendly and cost-effective materials towards sustainable dye-sensitized solar cells. *Green Chem.* **2020**, *22*, 7168–7218. [CrossRef]

13. Babu, D.D.; Naik, P.; Keremane, K.S. A simple D-A- $\pi$ -A configured carbazole based dye as an active photo-sensitizer: A comparative investigation on different parameters of cell. *J. Mol. Liquids* **2020**, *310*, 113189. [[CrossRef](#)]
14. An, J.; Yang, X.; Cai, B.; Zhang, L.; Yang, K.; Yu, Z.; Wang, X.; Hagfeldt, A.; Sun, L. Fine-Tuning by Triple Bond of Carbazole Derivative Dyes to Obtain High Efficiency for Dye-Sensitized Solar Cells with Copper Electrolyte. *ACS Appl. Mater. Interfaces* **2020**, *12*, 46397–46405. [[CrossRef](#)]
15. Alhorani, S.; Kumar, S.; Genwa, M.; Meena, P.L. Review of latest efficient sensitizer in dye-sensitized solar cells. In Proceedings of the Dae Solid State Physics Symposium 2019, Jodhpur, India, 18–22 December 2019.
16. Jung, I.H.; Kim, J.-H.; Nam, S.Y.; Lee, C.; Hwang, D.-H.; Yoon, S.C. Development of New Photovoltaic Conjugated Polymers Based on Di(1-benzothieno)[3,2-b:2',3'-d]pyrrole: Benzene Ring Extension Strategy for Improving Open-Circuit Voltage. *Macromolecules* **2015**, *48*, 5213–5221. [[CrossRef](#)]
17. Jung, I.H.; Kim, J.-H.; Nam, S.Y.; Lee, C.; Hwang, D.-H.; Yoon, S.C. A di(1-benzothieno)[3,2-b:2',3'-d]pyrrole and isoindigo-based electron donating conjugated polymer for efficient organic photovoltaics. *J. Mater. Chem. C* **2016**, *4*, 663–667. [[CrossRef](#)]
18. Zeng, W.D.; Cao, Y.M.; Bai, Y.; Wang, Y.H.; Shi, Y.S.; Zhang, M.; Wang, F.F.; Pan, C.Y.; Wang, P. Efficient Dye-Sensitized Solar Cells with an Organic Photosensitizer Featuring Orderly Conjugated Ethylenedioxythiophene and Dithienosilole Blocks. *Chem. Mater.* **2010**, *22*, 1915–1925. [[CrossRef](#)]
19. Ni, J.-S.; Yen, Y.-C.; Lin, J.T. Organic Dyes with a Fused Segment Comprising Benzotriazole and Thieno[3,2-b]pyrrole Entities as the Conjugated Spacer for High Performance Dye-Sensitized Solar Cells. *Chem. Commun.* **2015**, *51*, 17080–17083. [[CrossRef](#)]
20. Wu, Y.; Li, Y.; Gardner, S.; Ong, B.S. Indolo[3,2-b]carbazole-based thin-film transistors with high mobility and stability. *J. Am. Chem. Soc.* **2005**, *127*, 614–618. [[CrossRef](#)]
21. Wu, Y.; Zhu, W. Organic sensitizers from D- $\pi$ -A to D-A- $\pi$ -A: Effect of the internal electron-withdrawing units on molecular absorption, energy levels and photovoltaic performances. *Chem. Soc. Rev.* **2013**, *42*, 2039–2058. [[CrossRef](#)]
22. Yen, Y.S.; Chou, H.H.; Chen, Y.C.; Hsu, C.Y.; Lin, J.T. Recent developments in molecule-based organic materials for dye-sensitized solar cells. *J. Mater. Chem.* **2012**, *22*, 8734–8747. [[CrossRef](#)]
23. Xiao, Z.; Di, Y.; Tan, Z.; Cheng, X.; Chen, B.; Feng, J. Efficient organic dyes based on perpendicular 6,12-diphenyl substituted indolo[3,2-b]carbazole donor. *Photochem. Photobiol. Sci.* **2016**, *15*, 1514–1523. [[CrossRef](#)] [[PubMed](#)]
24. Xiao, Z.; Chen, B.; Di, Y.; Wang, H.; Cheng, X.; Feng, J. Effect of substitution position on photoelectronic properties of indolo[3,2-b]carbazole-based metal-free organic dyes. *Sol. Energy* **2018**, *173*, 825–833. [[CrossRef](#)]
25. Yao, Z.; Wu, H.; Li, Y.; Wang, J.; Zhang, J.; Zhang, M.; Guo, Y.; Wang, P. Dithienopicenocarbazole as the kernel module of low-energy-gap organic dyes for efficient conversion of sunlight to electricity. *Energy Environ. Sci.* **2015**, *8*, 3192–3197. [[CrossRef](#)]
26. Wang, E.; Yao, Z.; Zhang, Y.; Shao, G.; Zhang, M.; Wang, P. Significant Influences of Elaborately Modulating Electron Donors on Light Absorption and Multichannel Charge-Transfer Dynamics for 4-(Benzo[c][1,2,5]thiadiazol-4-yl ethynyl)benzoic Acid Dyes. *ACS Appl. Mater. Interfaces* **2016**, *8*, 18292–18300. [[CrossRef](#)] [[PubMed](#)]
27. Cabau, L.; Vijay Kumar, C.; Moncho, A.; Clifford, J.N.; López, N.; Palomares, E. A single atom change “switches-on” the solar-to-energy conversion efficiency of Zn-porphyrin based dye sensitized solar cells to 10.5%. *Energy Environ. Sci.* **2015**, *8*, 1368–1375. [[CrossRef](#)]
28. Xie, Y.; Tang, Y.; Wu, W.; Wang, Y.; Liu, J.; Li, X.; Tian, H.; Zhu, W.H. Porphyrin Cosensitization for a Photovoltaic Efficiency of 11.5%: A Record for Non-Ruthenium Solar Cells Based on Iodine Electrolyte. *J. Am. Chem. Soc.* **2015**, *137*, 14055–14058. [[CrossRef](#)] [[PubMed](#)]
29. Zhang, H.; Chen, Z.E.; Hu, J.; Hong, Y. Novel rod-shaped organic sensitizers for liquid and quasi-solid-state dye-sensitized solar cells. *Electrochim. Acta* **2019**, *295*, 934–941. [[CrossRef](#)]
30. Huang, Z.-S.; Feng, H.-L.; Zang, X.-F.; Iqbal, Z.; Zeng, H.; Kuang, D.-B.; Wang, L.; Meier, H.; Cao, D. Dithienopyrrolobenzothiadiazole-based organic dyes for efficient dye-sensitized solar cells. *J. Mater. Chem. A* **2014**, *2*, 15365–15376. [[CrossRef](#)]
31. Zang, X.-F.; Huang, Z.-S.; Wu, H.-L.; Iqbal, Z.; Wang, L.; Meier, H.; Cao, D. Molecular design of the diketopyrrolopyrrole-based dyes with varied donor units for efficient dye-sensitized solar cells. *J. Power Sources* **2014**, *271*, 455–464. [[CrossRef](#)]
32. Zhang, H.; Fan, J.; Iqbal, Z.; Kuang, D.-B.; Wang, L.; Meier, H.; Cao, D. Novel dithieno[3,2-b:2',3'-d]pyrrole-based organic dyes with high molar extinction coefficient for dye-sensitized solar cells. *Org. Electron.* **2013**, *14*, 2071–2081. [[CrossRef](#)]
33. Li, R.; Liu, J.; Cai, N.; Zhang, M.; Wang, P. Synchronously reduced surface states, charge recombination, and light absorption length for high-performance organic dye-sensitized solar cells. *J. Phys. Chem. B* **2010**, *114*, 4461–4464. [[CrossRef](#)]
34. Kitamura, T.; Ikeda, M.; Shigaki, K.; Inoue, T.; Anderson, N.A.; Ai, X.; Lian, T.; Yanagida, S. Phenyl-Conjugated Oligoene Sensitizers for TiO<sub>2</sub> Solar Cells. *Chem. Mater.* **2004**, *16*, 1806–1812. [[CrossRef](#)]
35. Qian, X.; Zhu, Y.-Z.; Chang, W.-Y.; Song, J.; Pan, B.; Lu, L.; Gao, H.-H.; Zheng, J.-Y. Benzo[a]carbazole-Based Donor- $\pi$ -Acceptor Type Organic Dyes for Highly Efficient Dye-Sensitized Solar Cells. *ACS Appl. Mater. Interfaces* **2015**, *7*, 9015–9022. [[CrossRef](#)] [[PubMed](#)]
36. Gao, X.; Li, Y.; Yu, L.; Hou, F.; Zhu, T.; Bao, X.; Li, F.; Sun, M.; Yang, R. The regulation of  $\pi$ -bridge of indacenodithiophene-based donor- $\pi$ -acceptor conjugated polymers toward efficient polymer solar cells. *Dyes Pigments* **2019**, *162*, 43–51. [[CrossRef](#)]
37. Zhong, Y.; Liu, D.; Zhang, K.; Li, Y.; Sun, M.; Yu, L.; Li, F.; Liu, H.; Yang, R. Modifying the morphology via employing rigid phenyl side chains achieves efficient nonfullerene polymer solar cells. *J. Polym. Sci. Part A Polym. Chem.* **2018**, *56*, 2762–2770. [[CrossRef](#)]

38. Wu, H.; Huang, Z.; Hua, T.; Liao, C.; Meier, H.; Tang, H.; Wang, L.; Cao, D.J.D. Metal-free organic dyes with di(1-benzothieno)[3,2-b:2',3'-d]pyrrole as a donor for efficient dye-sensitized solar cells: Effect of mono- and bi-anchors on photovoltaic performance. *Dyes Pigments* **2019**, *165*, 103–111. [[CrossRef](#)]
39. Vollbrecht, J.; Lee, J.; Ko, S.-J.; Brus, V.V.; Karki, A.; Le, W.; Seifrid, M.; Ford, M.J.; Cho, K.; Bazan, G.C.; et al. Design of narrow bandgap non-fullerene acceptors for photovoltaic applications and investigation of non-geminate recombination dynamics. *J. Mater. Chem. C* **2020**, *8*, 15175–15182. [[CrossRef](#)]
40. Lee, J.; Singh, R. Competitive role between conformational lock and steric hindrance in D-A copolymers containing 1,4-bis(thieno[3,2-b]thiophen-2-yl)benzene unit. *Dyes Pigments* **2020**, *181*, 108540. [[CrossRef](#)]
41. Fang, J.-K.; Hu, X.; Xu, M.; Wang, H.; Zhang, Y.; Jin, C.; Zhong, X. Molecular Engineering of Efficient Organic Sensitizers Containing Diyne-Bridge for Dye-Sensitized Solar Cells. *Electrochim. Acta* **2017**, *253*, 572–580. [[CrossRef](#)]
42. Huang, Z.S.; Zang, X.F.; Hua, T.; Wang, L.; Meier, H.; Cao, D. 2,3-Dipentylidithieno[3,2-f:2',3'-h]quinoxaline-based organic dyes for efficient dye-sensitized solar cells: Effect of  $\pi$ -bridges and electron donors on solar cell performance. *ACS Appl. Mater. Interfaces* **2015**, *7*, 20418–20429. [[CrossRef](#)] [[PubMed](#)]
43. Wu, Y.; Zhang, Q.; Li, J.; Tian, X.; Li, D.; Lu, X.; Xu, B.; Wu, Y.; Guo, K. Regulation of dithiafulvene-based molecular shape and aggregation on TiO<sub>2</sub> for high efficiency dye-sensitized solar cells. *J. Mater. Chem. C* **2019**, *7*, 1974–1981. [[CrossRef](#)]
44. Pei, K.; Wu, Y.; Islam, A.; Zhang, Q.; Han, L.; Tian, H.; Zhu, W. Constructing high-efficiency D-A-pi-A-featured solar cell sensitizers: A promising building block of 2,3-diphenylquinoxaline for antiaggregation and photostability. *ACS Appl. Mater. Interfaces* **2013**, *5*, 4986–4995. [[CrossRef](#)] [[PubMed](#)]
45. Huang, Z.-S.; Hua, T.; Tian, J.; Wang, L.; Meier, H.; Cao, D. Dithienopyrrolobenzotriazole-based organic dyes with high molar extinction coefficient for efficient dye-sensitized solar cells. *Dyes Pigments* **2016**, *125*, 229–240. [[CrossRef](#)]